

Cyclopia in a newborn rhesus macaque born to a dam infected with SIV and receiving antiretroviral therapy during pregnancy

Lara Doyle-Meyers¹, Chunming Dong², Eddie Qidi Xu^{2,3}, Eric J. Vallender^{1,4}, Robert V. Blair^{5,6}, Peter Didier^{5,6}, Fenglei He^{2,#} and Xiaolei Wang^{5,6,#,*}

¹Division of Veterinary Medicine, Tulane National Primate Research Center, 18703 Three Rivers Road, Covington, LA, 70433, USA; ²Department of Cell and Molecular Biology, School of Science and Engineering, Tulane University, 6823 St. Charles Avenue, New Orleans, LA, 70118, USA;

³Tulane University School of Public Health and Tropical Medicine, 1440 Canal Street, New Orleans, LA, 70112, USA; ⁴Department of Psychiatry and Human Behavior, Division of Neurobiology and Behavior Research, University of Mississippi Medical Center, Jackson, MS, 39216, USA;

⁵Pathology & Laboratory Medicine, Tulane University School of Medicine, 1430 Tulane Avenue, New Orleans, LA, 70112, USA; ⁶Division of Comparative Pathology, Tulane National Primate Research Center, 18703 Three Rivers Road, Covington, LA, 70433, USA.

ABSTRACT

Cyclopia, a rare genetic anomaly and birth defect, was recently observed in our nonhuman primate study. A newborn rhesus macaque, delivered *via* cesarean section, exhibited facial abnormalities, including a single eye in the middle of the forehead. This macaque was born to a dam who had been inoculated with SIV in the first trimester and received antiretroviral therapy (ART) in the early third trimester of pregnancy. Prenatal ultrasound detected fetal defects, including the fusion of the thalami and absence of third ventricle during the third trimester of fetal development. Remarkably, the newborn macaque was diagnosed with severe alobar holoprosencephaly, characterized by a single eye located on the facial midline and proboscises positioned above and below the eye. This condition was accompanied by the absence of a nose, mouth, mandible, maxilla, nasal and oral cavities, tongue, as well as the esophagus.

Subsequent genetic screening identified a significant down-regulation of craniofacial development-associated genes, although genetic mutations in the sonic hedgehog gene (*SHH*) were not present. As the fetal defects were identified prior to the initiation of antiretroviral therapy, it is possible that other environmental factors may have contributed to the development of cyclopia in this rhesus case. However, the etiology of this congenital HPE case remains essentially unknown.

KEYWORDS: holoprosencephaly, cyclopia, newborn, rhesus macaque, genetic screening.

INTRODUCTION

During embryogenesis in the womb, the prechordal mesoderm develops the median facial bones and induces the rostral neuroectodermal differentiation. Primary neurulation is responsible for the formation of the neural tube, which gives rise to forebrain, midbrain and hindbrain during the first weeks of gestation [1]. Neural tube defects occurring at this stage lead to cyclopia and other forms of holoprosencephaly (HPE) due to the

*Corresponding author: xwang@tulane.edu

#Equal contribution.

absence or incomplete separation of the forebrain into the right/left hemispheres and lobes [2-5]. HPE consists of alobar, semi-lobar, lobar and middle interhemispheric variant subtypes, characterized by severe brain defects (failures of hemisphere cleavage with a single brain ventricle), moderate form of the disorders (partial division of the hemisphere), minor structural defects (partial frontal horn and absence of the corpus) or fused middle hemisphere [6-10], resulting in severe facial defect [4, 11]. Among these subtypes, cyclopia is the most severe form of HPE, presenting as the alobar type, occurring in 1 in 100,000 live and stillbirths. It is often associated with anophthalmia, cyclopia, ethmocephaly, and/or microphthalmia and may include a proboscis [12]. This congenital malformation usually occurs between the 18 and 28 days of gestation in humans, prior to the lateral movement of the optic primordia [13-15].

In our recent nonhuman primate study, a newborn macaque born to an SIV-infected dam was diagnosed with cyclopia. To our knowledge, this is the first reported case of cyclopia with agnathia-otocephaly in an Indian-origin rhesus macaque (*Macaca mulatta*). Here, we retrospectively tracked the longitudinal ultrasound screenings during pregnancy, characterized the syndrome in this specific cyclopia case, and examined pathological changes and potential genetic alterations.

MATERIALS AND METHODS

Ethics statement

All animals in this study were housed at the Tulane National Primate Research Center in accordance with the Association for Assessment and Accreditation of Laboratory Animal Care International standards. All studies were reviewed and approved by the Tulane University Institutional Animal Care and Use Committee under protocol number P0408. Animal housing and studies were carried out in strict accordance with the recommendations in the Guide for the Care and Use of Laboratory Animals of the National Institutes of Health (NIH, AAALAC #000594). All clinical procedures were carried out under the direction of a laboratory animal

veterinarian. All procedures were performed under anesthesia, and all efforts were made to minimize stress, improve housing conditions, and to provide enrichment opportunities (e.g., objects to manipulate in cage, varied food supplements, foraging and task-oriented feeding methods, interaction with caregivers and research staff).

Animal and necropsy

The affected fetus was born *via* a cesarean section (c-section) to an eight-year-old female rhesus macaque. The dam was from the Tulane National Primate Research Center's (TNPRC) specific pathogen free (SPF) 4 colony and had two healthy infants prior to this pregnancy. The dam was determined to be in her first trimester of pregnancy during her semi-annual health assessment in the TNPRC's breeding colony. She was assigned to the study and infected with Simian Immunodeficiency Virus (SIV) mac 251 on approximately 25 days of gestational age (dGA). One week later, the dam developed diarrhea and a rectal culture was performed to test enteric pathogens. The culture was positive for *Pseudomonas aeruginosa* and *Campylobacter coli* and *jejuni*. She was treated with azithromycin for five days. The diarrhea resolved and the rest of the pregnancy was unremarkable.

Amniocenteses and fetal measurements *via* ultrasonography were performed and collected monthly. A c-section was performed at approximately 158 dGA. After the infant was removed from the uterus and the full extent of his condition was discovered, the infant was euthanized immediately. An exam of the infant, including measurements and photographs, was performed post-mortem. A gross necropsy was performed, and tissues were collected for histopathological analysis.

Sample RNA and genomic DNA extraction for viral measurement and genetic screening

PBMC or splenocytes ($\sim 10^7$ in total per samples) were processed to extract cellular genomic DNA and cellular RNA with a AllPrep DNA/RNA Mini Kit (Cat No: 80311, Qiagen) according to the manufacturer's instructions. Viral RNA in plasma was directly isolated using the QIAamp Viral RNA Mini Kit (Cat No: 52962, Qiagen). The

extracted DNA and RNA samples were stored at -80 °C for further use.

Quantitative polymerase chain reaction (PCR) measurement: 0.5 µg of RNA was used for 20 µL cDNA synthesis, employing the Script cDNA Synthesis Kit (Bio-Rad Laboratories). Subsequently, 4 µL of diluted cDNA samples (1:5 in dH₂O) were utilized for the PCR reaction. Quantification of cyclopia-related genes was conducted on the Bio-Rad iCycler, employing SYBR Green PCR Master Mix (Applied Biosystem). The following amplification conditions were applied: an initial denaturation at 95°C for 10 minutes, followed by 40 cycles of denaturation at 95°C for 15 seconds and annealing/extension at 60°C for 1 minute. The

cycle threshold (Ct) values for each gene were normalized to the housekeeping gene GAPDH. SIV and cytomegalovirus (CMV) in plasma were examined using QuantStudio Absolute Q digital PCR system (Thermo Fisher Scientific). The primers and probes used are shown in Table 1.

Genomic sequencing and analysis: Whole-genome sequencing was conducted on an Illumina NovaSeq 6000 (Foster City, CA). The genome was aligned to the Mmul_10 reference genome [16] using the Burrows–Wheeler Aligner [17] and processed following best practice recommendations from the Broad Institute using the Genome Analysis Toolkit [18, 19] following pipelines established for the macaque Genotype And

Table 1. Primers/Probes used to quantify cyclopia-related genes and viruses.

Gene	Primer	Sequence (5' to -3')
GAPDH	GAPDH-ma-F	CCTCCTGTTCGAGAGTCAGC
	GAPDH-ma-R	CCCAATACGACCAAATCCGTTG
Gli1	Gli1-ma-F	GCCCAGACAGAGTGTCCC
	Gli1-ma-R	GCCATAGCTACTGACTGGTGG
Gli2	Nkx2-2-ma-F	CCGCGCTCCAGGTTCTGT
	Nkx2-2-ma-R	GGCGTCAGCTTGGGCTC
Nkx2-2	FoxA2-ma-F	TGCACTCGGCTTCCAGTA
	FoxA2-ma-R	GGAGGAGTAGCCCTCGG
FoxA2	Gli2-ma-F	GTAAGCAGGAGGCTGAGGTG
	Gli2-ma-R	GCTCGTTGTTGATGTGGTGC
GAS1	GAS1-ma-F	CGCTACCTAACCTACTGCGG
	GAS1-ma-R	CACACGCAGTCATTGAGCAG
Shh	Shh-ma-F	GCTCGGTGAAAGCAGAGAAC
	Shh-ma-R	GTCCTTTACCAGCTTGGTGC
Rhesus CMV	RhCMVF	GTTTAGGGAACCGCCATTCTG
	RhCMVR	GTATCCGCGTTCCAATGCA
	RhCMVP	FAM-TCCAGCCTC/ZEN/CATAGCCGGGAAGG-BHQ
SIV	SIV gag-F	GTCTGCGTCATCTGGTGCATTC
	SIV gag-R	CACTAGGTGTCTCTGCACTATCTGTTTTG
	SIV gag-P	FAM-CTTCCTCAGTGTTTCACTTTCTCTTCTGCG-3IABKFQ-1

Phenotype (mGAP) resource [20]. Data was submitted to the NIH Sequence Read Archive as SAMN28555554. Genomic data can also be obtained at mGAP (<http://mgap.ohsu.edu>) with the sample ID 'm08233'.

RESULTS

Prenatal ultrasound screening of fetus during pregnancy

Indian rhesus macaques (*Macaca mulatta*) have marked gestational period similarities to humans from puberty to menopause [21, 22]. Female macaques reach puberty around 3 years of age and can reproduce until 20 years of age. Their gestation period ranges from 158 to 173 days (average 166.5 days), and fetus is considered as the prenatal stage between late stage of 1st trimester and birth [23]. The rhesus dam was intravenously inoculated with SIVmac251 at 25 dGA during the first trimester and received 1.5 months of combined antiretroviral therapy, which began at 113 dGA at the early third trimester. The newborn was delivered by C-section at 158 dGA (Figure 1A). In this case, the first age of the fetus was estimated by fetal length measurement at 18 dGA. Additional ultrasound measurements of various parameters were conducted monthly (Table 2). The ultrasound images showed that the thalami and third ventricle were still detectable at 53 and 81 dGA. However, starting at three months post SIV inoculation (109 dGA), the fetal head became progressively smaller compared to other parameters, including femur length and abdominal circumference, and the thalami appeared fused with the third ventricle and no longer visible, despite a normal heart rate (HR) throughout the pregnancy (Figure 1B). During the C-section (158 dGA), it was noted that the uterus appeared large and flaccid and contained an excessive amount of yellow amniotic fluid.

Clinical evaluation

The male neonate weighed 330 grams. A physical examination was conducted shortly after euthanasia. This newborn exhibited a single midline orbit containing a single eyeball, with two small fleshy pedunculated masses appearing as proboscises above and below the central eye. There was a lack of nose, nostrils, oral cavity,

penis, testes, tongue, and esophagus. Generally, the scrotum appeared relatively smaller than in other male neonates born at the center, and a penile shaft was not appreciated upon physical examination (Figure 2A). The proboscis below the eye was slightly larger than the one above the eye, serving as a replacement for a functioning nose (Figure 2B). In humans, this form of cyclopia is termed rhinocephaly, where the proboscis is typically found above the central eye [24, 25]. On the other hand, the maxillary and mandibular bones were essentially absent (Figure 2C). A tight transverse aperture lined by thin lip structures, possibly a remnant of the mouth, was located below the eye and opened into a subcutaneous recess devoid of a pharynx and esophagus (Figure 2D). The ears were positioned ventromedially on his head (Figure 2D).

Brain pathology

Cyclopia is characterized by the absence of right/left hemisphere cleavage, maldevelopment of embryonic forebrain, and aberrant formation of two orbits [26]. Indeed, the cranium was small and flattened on the dorsal-ventral axis, attributed to the loss of neuropile in the frontal, temporal, and parietal lobes, along with the expansion of lateral ventricle spaces (Figure 3A). The midbrain and medulla were compressed, with an opening in the neural tube at the commissure of the inferior colliculi. Average neonatal measurements post-mortem included biparietal diameter (BPD) of 39.5 mm, occipitofrontal diameter of 49.5 mm, crown-rump length of 190.5 mm, abdominal circumference of 115.5 mm, thoracic circumference of 120 mm, humeral length of 50 mm, and femoral length (FL) of 55 mm. Comparison of BPD and FL to published fetal standards estimated gestation days between 112 (BPD) and >165 (FL) [27], with this fetal weight being 33% less than expected at term [28]. Microscopically, the cerebral cortex exhibited reduced numbers of disorganized and sometimes pyknotic neurons, increased glial cells, and expansion of the lateral ventricular space in the parietal and temporal lobes (Figures 3B-3D).

Eye pathology

The striking anomaly in this neonate was a single eye in the mid-forehead (cyclopia). The single eye

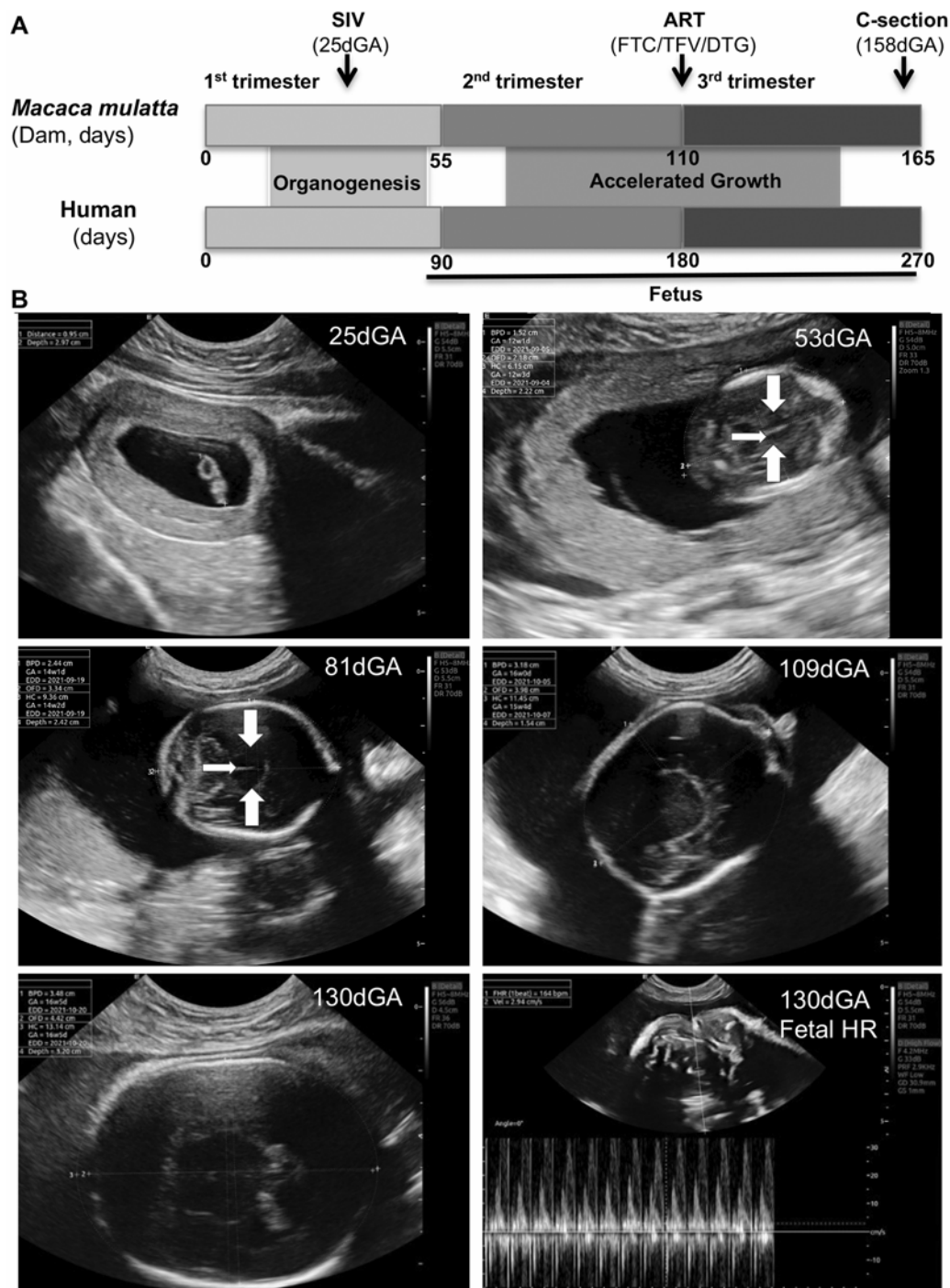


Figure 1. Similarities of gestational period between human and rhesus macaques and the study of pregnant rhesus macaque during pregnancy. (A) Duration of gestation in rhesus macaques compared to humans, along with details of the animal study regarding SIV inoculation and antiretroviral therapy. Each trimester represents a different period of pregnancy, characterized by organogenesis, and accelerated fetal development. **(B)** Ultrasound screening during pregnancy. Ultrasound scans were performed at 25, 53, 81, 109, and 130 dGA. In the axial view of the fetal head in the transthalamic plane, thalami (thick arrow) and the third ventricle (thin arrow) remained identifiable at earlier stages (53 and 81dGA) but were no longer visible at 109 or 130 dGA. Note that the dam had not received antiretroviral therapy at 109 dGA. dGA, day of gestation; HR, heart rate.

Table 2. Fetal measurements and ultrasound screening assessment during pregnancy.

Date (Ultrasound screening)	dGA	HR	GL (mm)	BPD (mm)	OFD (mm)	HC (mm)	AC (mm)	FL(A) (mm)	FL(B) (mm)	dGA (Equivalent to healthy fetus)
1/19/2021	18									
1/26/2021	25	152	8.9							30-31
2/23/2021	53	196		15.1	21.9	61		5.3	7.3	55-56 (head); 56-57 (femur A); 61-62 (femur B)
3/23/2021	81	182		24.5	33.9	94.7	97.4	16.5	17.3	74-75 (head); 82-85 (femur); 85 (AC)
4/20/2021	109	175		31.5	41.7	120	123	28.1	27.4	89-90 (head); 108-111 (femur); 106 (AC)
5/11/2021	130	164		34.3	44.7	131	131	34.8	34.4	95-98 (head); 127-129 (femur); 114 (AC)
6/8/2021 Post-cesarean section	158	146	190.5 (crown-rump)	39.5 (GD 112-113)	49.5	145 (GD 104)	115.5 (GD 99)	55 (GD >165)	55 (GD >165)	

All data were collected via ultrasound examination except for the data at the time of C-section (highlighted in gray which were collected post-cesarean section). The heart rate was collected via ultrasound examination on 158 dGA. dGA, days of gestation; HR, heart rate; GL, gestational length; BPD, biparietal diameter; OFD, occipital-frontal diameter; HC, head circumference; AC, abdominal circumference; FL, femur length; and mm, millimeters.

exhibited a normal-appearing sclera (Figures 4A and 4B.1), cornea (Figures 4A and 4B.2), iris (Figures 4A and 4B.3), and ciliary body (Figures 4A and 4B.4), but lenticular (Figure 4C) and retinal (Figures 4D-4F) dystrophy. Dystrophic changes in the lens were consistent with cataract characterized by liquefaction of lens proteins and formation of Morgagnian globules (Figure 4C). Retinal dystrophy was characterized by widespread vacuolation of the nerve fiber layer (Figure 4E) and multifocal rosettes in the outer nuclear layer with thinning and loss of the inner nuclear and plexiform layers (Figure 4F).

Genetic screening

There are at least ten genes implicated in the HPE phenotype in humans, and their abnormal expression or defects result in maldevelopment of the early forebrain [2, 29-34]. These include SHH, SIX3, ZIC2, TGIF [35-37], PTCH1 [38], GLI2 [39], CDON [40], CNOT1 [41], STAG2 [42], PLCH1 [43] associated with HPE, as well as an additional two genes, PRRX1 [44] and OTX2 [45], in agnathia-otocephaly. Genomic sequence analysis revealed that the animal cyclopia case did not harbor any unique polymorphisms, or any frameshift, missense, or nonsense mutations, or

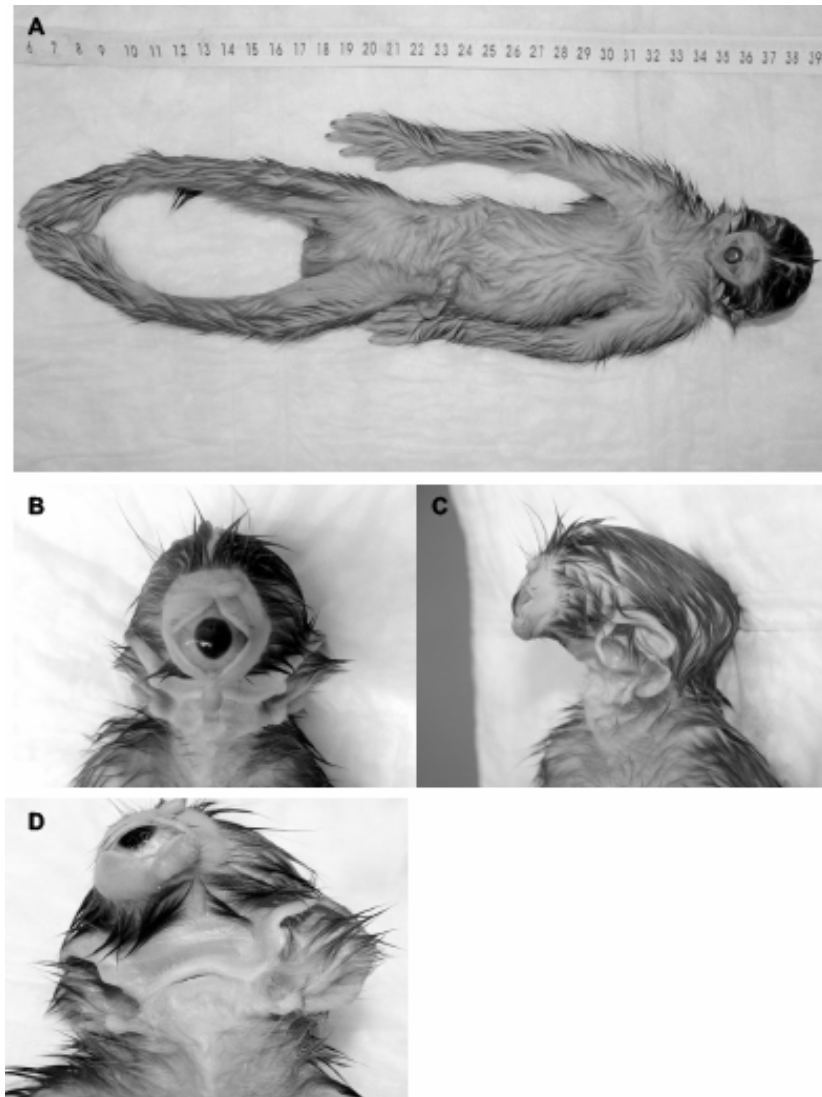


Figure 2. Overview of the body, face, eye, and ears of the newborn macaque. (A) The entire body in dorsal recumbency. The newborn macaque displayed a single eye with proboscises situated both above and below the eye. Notably, there was an absence of the nose, penis, testes, mouth, mandible, maxilla, nasal and oral cavities, tongue, as well as the esophagus. (B) Proboscises were positioned both above and below the eye. (C) Lateral view of the newborn's face. Both the mandible and maxilla were absent. (D) A transverse aperture was lined by thin lip structures, and the ears were located ventromedially.

any other mutations predicted to be deleterious in these 12 genes. Putative regulatory regions homologous to those identified in mouse and previously associated with midline defects [46-48] were also identified in the rhesus macaque Mmul_10 reference genome [16]: SBE1 chr3:181802672-181803199, SBE2 chr3:182272629-182273783, SBE3 chr3:182310077-182310487, SBE4 chr3:182141002-182142174, and SBE7 chr3:

182331104-182331969. These brain distal enhancer regions for SHH had no unique or even rare mutations in the case animal. Despite the lack of identifiable mutations in the cyclopia case, expression of craniofacial development-related genes, including SHH and Gli1, was downregulated in the specimen of cyclopia case compared to the age-matched healthy control. These findings were consistent with the decreased

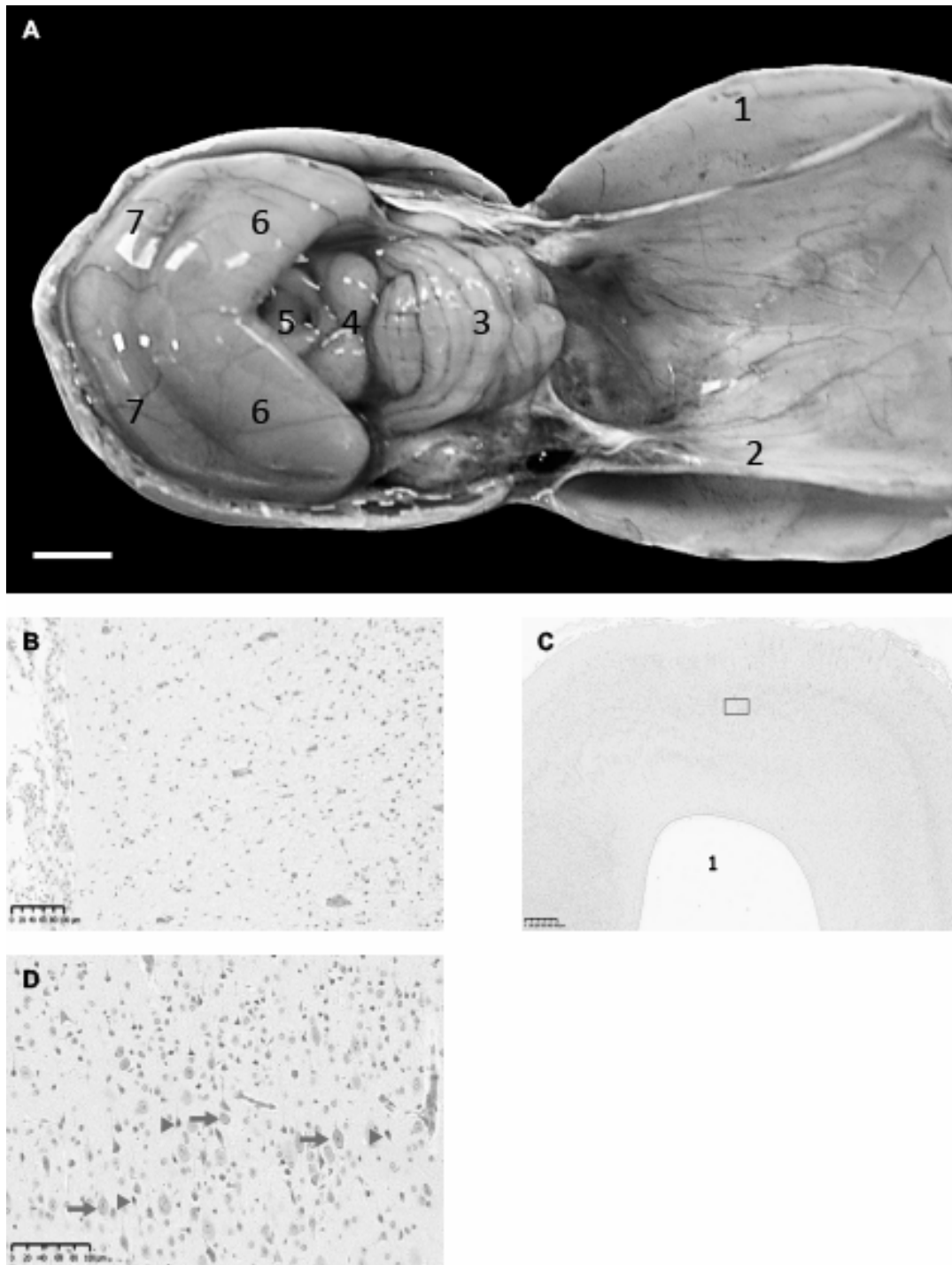


Figure 3. Brain and lobes of newborn macaque. (A) The fetal brain is depicted, including the cranium (1), meninges (2), cerebellum (3), midbrain (4), neural tube (5), occipital (6), and parietal (7) lobes. Scale bar = 1 cm. It's important to note that the cerebellum is slightly flattened, the midbrain appears normal, but the ventricular space is dilated, the neural tube is open, and the occipital and parietal lobes are reduced in size. (B) The frontal lobe is smaller than normal and lacks neuronal layers. (C) The parietal lobe displays a dilated lateral ventricle lined by ependymal cells (1) and disorganized neural layers. (D) The inner parietal lobe (boxed area in C) exhibits disorganized neurons (arrows) and degenerated neurons (arrowheads).

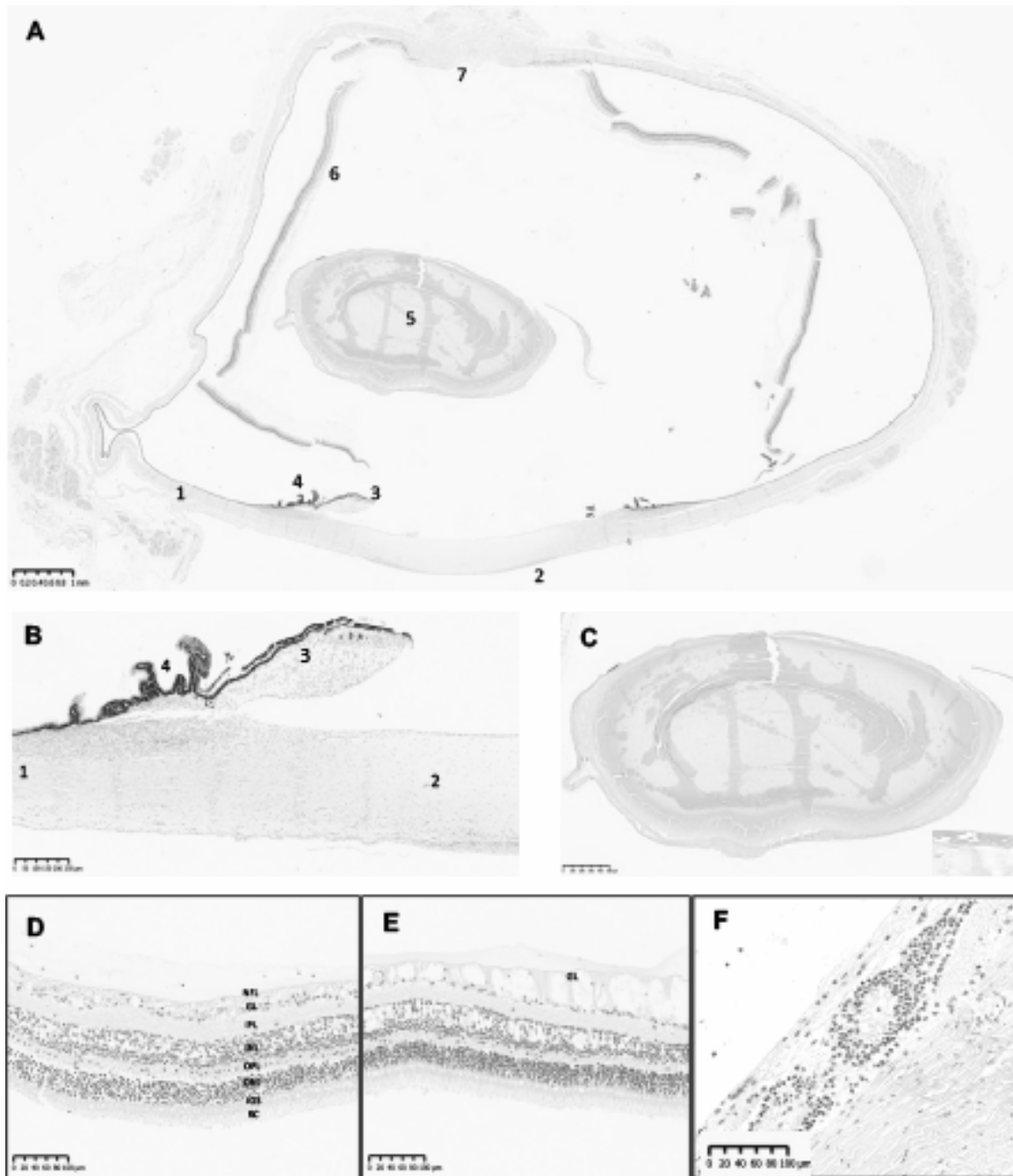


Figure 4. Pathology of the single eye in the neonatal macaque cyclopia case. (A) The cyclopean eye is displayed, highlighting its typical components, including the sclera (1), cornea (2), iris (3), ciliary body (4), lens (5), retina (with artifactual processing detachment and fragmentation) (6), and optic disc (7). (B) Anatomical structures of the eye are depicted, featuring the sclera (1), cornea (2), iris (3), and ciliary body (4). (C) The lens exhibits pale areas indicative of cataractous change. Inset: High magnification demonstrating liquefaction of lens proteins and Morgagnian globule formation. (D) The retina comprises all the expected layers, including the nerve fiber layer (NFL), ganglion layer (GL), inner plexiform layer (IPL), inner nuclear layer (INL), outer plexiform layer (OPL), outer nuclear layer (ONL), inner and outer segments (IOS), and rods and cones (RC). (E) Segmental hydropic degeneration of the nerve fiber layer of the retina is observed. (F) Retinal rosettes are rarely noted in the outer nuclear layer, with variable thinning and loss of other retinal layers adjacent to the rosettes.

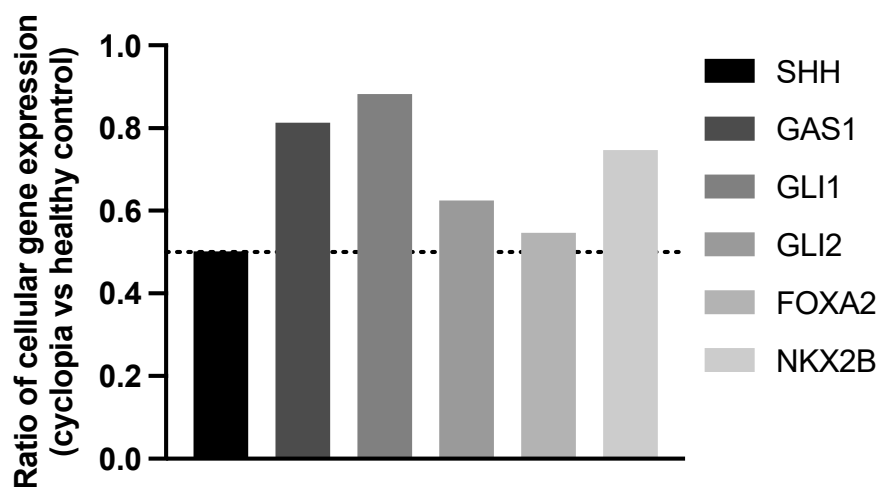


Figure 5. Quantification of *SHH*, *GAS1*, *GLI1*, *GLI2*, *FOXA2*, and *NKX2B* mRNA in specimens of newborn macaques cyclopia case. Cyclopia-related genes were normalized using the housekeeping gene GAPDH and compared between specimens of the cyclopia case and an age-matched healthy animal. The comparative expression of sonic hedgehog (*SHH*) and related genes in the affected newborn macaque were presented as a ratio compared to healthy animal control. The data represent at least three independent measurements.

levels observed in other downstream targets of the *SHH* signaling pathway, including *GAS1*, *GLI2*, *FOXA2*, and *NKX2B* (Figure 5).

DISCUSSION

Cyclopia is a heterogeneous syndrome that is associated with genetic defects, environmental factors, and infectious diseases [8, 24, 49]. The most common chromosomal disorder linked to HPE is trisomy 13, also known as Patau Syndrome [8, 14, 50]. The sonic hedgehog (*SHH*) gene on chromosome 7 was the first reported gene known to cause human HPE [2, 51]. This gene encodes a protein found in the prechordal mesoderm and notochord, responsible for early forebrain development. When a mutation in the *SHH* gene occurs, the downstream signaling pathway is disrupted, leading to HPE phenotypes [2, 29-34]. In this report, no putative pathogenic mutations were detected in *SHH* or any other gene associated with HPE in humans. Likewise, no suggestive mutations were detected in the putative distal enhancer regions of *SHH*. Despite this, expression of genes associated with cyclopia and craniofacial maldevelopment, including *SHH*, were significantly downregulated in specimen of the macaque cyclopia case compared to those from a healthy control. Although it remains

unknown why *SHH* is significantly downregulated in this newborn rhesus cyclopia case, it is likely that reduced expression of *SHH* contributes to the holoprosencephaly. We also examined trisomies in this animal, and no chromosomal aneuploidy was found. The dam has no obstetric history of a teratogenic outcome, as previous pregnancies resulted in normal and healthy newborns, and HPE generally does not correlate with maternal age [52, 53].

In addition to genetic causes, environmental factors and infectious diseases are also implicated in HPE. Maternal exposure to alcohol, retinoic acid, lithium, salicylates, and other chemicals, or maternal diabetes during pregnancy, poses a high risk of HPE [8, 54-58]. Indeed, exposure to alcohol [59], an anti-progestational agent [60] in pigtail or cynomolgus macaques during pregnancy may induce mutagenic effects. In our pregnant rhesus macaque studies, the dam was not persistently exposed to chemicals or drugs during pregnancy according to the history of animal care. Furthermore, TORCH (an acronym representing *Toxoplasma gondii*, other agents, rubella, cytomegalovirus, and herpes simplex virus) infection during early pregnancy can potentially cause neurological embryogenesis and subsequent holoprosencephaly [61-63], yet these infectious

pathogens, or gestational diabetes were negative in this dam. Cyclopia was observed in only one out of eighteen newborn macaques born to dam cohorts when dams were inoculated with SIV at first trimester, with or without ART exposure. Notably, on digital PCR detection this newborn tested negative for both SIV RNA and cytomegalovirus (CMV) DNA in plasma. Given that fetal defects were identified by ultrasound screening beginning at 81-109dGA at early third trimester, prior to the initiation of ART in the dam, maldevelopment of this fetus is not likely associated with exposure antiretroviral drugs. While a potential risk factor, maternal SIV exposure during pregnancy are not excluded due to limited number of pregnant macaques, yet the incidence of HPE is considered not to be linked to maternal HIV infection [2]. Collectively, the exact etiology of this congenital HPE case remains essentially unknown.

CONCLUSION

A newborn macaque, born to an SIV-infected dam, displayed severe alobar holoprosencephaly, characterized by a typical cyclopia including a single eye in the middle of the forehead and proboscises. This uncommon congenital defect case offers insights into the potential impact of maternal HIV infection on birth defects and abnormal infant development. It underscores the importance of studying HIV and antiretroviral exposure during pregnancy for research on craniofacial development, especially concerning human health implications.

ACKNOWLEDGMENTS

This work was supported by National Institutes of Health grants R01 AI147372, R01 HD099857, P51 OD011104, U42 OD024282, U42 OD010568 and R24 OD021324.

CONFLICT OF INTEREST STATEMENT

The authors declare no competing financial interests.

ABBREVIATIONS

ART : Antiretroviral therapy
 PCR : Polymerase chain reaction
 C-section : Cesarean section

dGA : Days of gestational age
 SHH : Sonic hedgehog
 HPE : Holoprosencephaly
 HR : Heart rate
 BPD : Biparietal diameter
 FL : Femoral length

REFERENCES

1. Winter, T. C., Kennedy, A. M. and Woodward P. J. 2015, *Radiographics*, 35, 275.
2. Dubourg, C., Bendavid, C., Pasquier, L., Henry, C., Odent, S. and David, V. 2007, *Orphanet. J. Rare. Dis.*, 2, 8.
3. Nyberg, D. A., Mack, L. A., Bronstein, A., Hirsch, J. and Pagon, R. A. 1987, *AJR Am. J. Roentgenol.*, 149, 1051.
4. Demyer, W. and Zeman, W. 1963, *Confin. Neurol.*, 23, 1.
5. Cohen, M. M. Jr. 2006, *Birth Defects Res. A. Clin. Mol. Teratol.*, 76, 658.
6. Demyer, W., Zeman, W. and Palmer, C. G. 1964, *Pediatrics*, 34, 256.
7. Kallen, B., Castilla, E. E., Lancaster, P. A., Mutchinick, L. B., Martnex-Frias, M. L., Mastroiacovo, P. and Robert, E. 1992, *J. Med. Genet.*, 29, 30.
8. Orioli, I. M., Amar, E., Bakker, M. K., Bermejo-Sanchez, E., Bianchi, F., Canfield, M. A., Clementi, M., Correa, A., Csaky-Szunyogh, M., Feldkamp, M. L., Landau, D., Leoncini, E., Li, Z., Lowry, R. B., Mastroiacovo, P., Morgan, M., Mutchinick, O. M., Rissmann, A., Rivanen, A., Scarano, G., Szabova, E. and Castilla, E. E. 2011, *Am. J. Med. Genet. C. Semin. Med. Genet.*, 157C, 344.
9. Hong, M. and Krauss, R. S. 2017, *PLoS One*, 12, e0176440.
10. Roessler E., Hu, P. and Muenke, M. 2018, *Am. J. Med. Genet. C. Semin. Med. Genet.*, 178, 165.
11. Solomon, B. D., Kruszka, P. and Muenke, M. 2018, *Am. J. Med. Genet. C. Semin. Med. Genet.*, 178, 117.
12. Diogo, R., Razmadze, D., Siomava, N., Douglas, N., Fuentes, J. S. M. and Duerinckx, A. 2019, *Sci. Rep.*, 9, 991.

13. Shiota, K., Yamada, S., Komada, M. and Ishibashi, M. 2007, *Am. J. Med. Genet. A.*, 143A, 3079.
14. Matalliotakis, M., Trivli, A., Matalliotaki, C., Moschovakis, A. and Hatzidaki, E. 2021, *Cureus*, 13, e17114.
15. Roach, E., Demyer, W., Conneally, P. M., Palmer, C. and Merritt, A. D. 1975, *Birth. Defects. Orig. Artic. Ser.*, 11, 294.
16. Warren, W. C., Harris, R. A., Haukness, M., Fiddes, I. T., Murali, S. C., Fernandes, J., Dishuck, P. C., Storer, J. M., Raveendran, M., Hillier, L. W., Porubsky, D., Mao, Y., Gordon, D., Vollger, M. R., Lewis, A. P., Munson, K. M., DeVogelaere, E., Armstrong, J., Diekhans, M., Walker, J. A., Tomlinson, C., Graves-Lindsay, T. A., Kremitzki, M., Salama, S. R., Audano, P. A., Escalona, M., Maurer, N. W., Antonacci, F., Mercuri, L., Maggiolini, F. A. M., Catacchio, C. R., Underwood, J. G., O'Connor, D. H., Sanders, A. D., Korbel, J. O., Ferguson, B., Kubisch, H. M., Picker, L., Kalin, N. H., Rosene, D., Levine, J., Abbott, D. H., Gray, S. B., Sanchez, M. M., Kovacs-Balint, Z. A., Kemnitz, J. W., Thomasy, S. M., Roberts, J. A., Kinnally, E. L., Capitanio, J. P., Skene, J. H. P., Platt, M., Cole, S. A., Green, R. E., Ventura, M., Wiseman, R. W., Paten, B., Batzer, M. A., Rogers, J., Eichler, E. E. 2020, *Science*, 370, abc6617.
17. Li, H. and Durbin, R.. 2010, *Bioinformatics*, 26, 589.
18. McKenna, A., Hanna, M., Banks, E., Sivachenko, A., Cibulskis, K., Kernytzky, A., Garimella, K., Altshuler, D., Gabriel, S., Daly, M. and DePristo M. A. 2010, *Genome Res.*, 20, 1297.
19. van der Auwera, G. A., Carneiro, M. O., Hartl, C., Poplin, R., Del Angel, G., Levy-Moonshine, A., Jordan, T., Shakir, K., Roazen, D., Thibault, J., Banks, E., Garimella, K., Altshuler, D., Gabriel, S. and DePristo, M. A. 2013, *Curr. Protoc. Bioinformatics*, 43, 11.10.11.
20. Bimber, B. N., Yan, M. Y., Peterson, S. M., and Ferguson, B. 2019, *BMC Genomics*, 20, 176.
21. Abel, K. 2009, *Curr. HIV Res.*, 7, 2.
22. Stouffer, R. L. and Woodruff, T. K. 2017, *ILAR J.*, 58, 281.
23. Kumar, V., Raj, A. and Kumar, P. 2011, *Open Vet. J.*, 1, 32.
24. Kunwar, A., Shrestha, B. M., Shrestha, S., Paudyal, P. and Rawal, S. 2021, *Clin. Case Rep.*, 9, e04466.
25. Sharma, D., Yadav, J. and Garg, E. 2014, *BMJ Case Rep.*, 2014.
26. Cannistra, C., Barbet, P., Parisi, P. and Iannetti, G. 2001, *J. Craniomaxillofac. Surg.*, 29, 150.
27. Tarantal, A. F. and Hendrickx, A. G. 1988, *J. Med. Primatol.*, 17, 105.
28. Digiacomo, R., Shaughnessy, P. W. and Tomlin, S. L. 1978, *Biol. Reprod.*, 18, 749.
29. Chen, C. P., Chern, S. R., Lee, C. C., Chen, L. F., Chuang, C. Y. and Chen, M. H. 1998, *Prenat. Diagn.*, 18, 393.
30. Traboulsi, E. I. 1998, *J. AAPOS.*, 2, 317.
31. Golden, J. A., Bracilovic, A., McFadden, K. A., Beesley, J. S., Rubenstein, J. L. and Grinspan, J. B. 1999, *Proc. Natl. Acad. Sci. USA*, 96, 2439.
32. Ohuchi, H., Sato, K., Habuta, M., Fujita, H. and Bando, T. 2019, *Congenit. Anom. (Kyoto)*, 59, 56.
33. Xu, J., Iyyanar, P. P. R., Lan, Y. and Jiang, R. 2023, *Differentiation*, 133, 60.
34. Dale, J. K., Vesque, C., Lints, T. J., Sampath, T. K., Furley, A., Dodd, J. and Placzek, M. 1997, *Cell*, 90, 257.
35. Dubourg, C., Lazaro, L., Pasquier, L., Bendavid, C., Blayau, M., Le Duff, F., Durou, M. R., Odent, S. and David, V. 2004, *Hum. Mutat.*, 24, 43.
36. Nanni, L., Ming, J. E., Bocian, M., Steinhaus, K., Bianchi, D. W., Die-Smulders, C., Giannotti, A., Imaizumi, K., Jones, K. L., Campo, M. D., Martin, R. A., Meinecke, P., Pierpont, M. E., Robin, N. H., Young, D., Roessler, E. and Muenke, M. 1999, *Hum. Mol. Genet.*, 8, 2479.
37. Wallis, D. and Muenke, M. 2000, *Hum. Mutat.*, 16, 99.
38. Ming, J. E., Kaupas, M. E., Roessler, E., Brunner, H. G., Golabi, M., Tekin, M., Stratton, R. F., Sujansky, E., Bale, S. J. and Muenke, M. 2002, *Hum. Genet.*, 110, 297.

39. Roessler, E., Du, Y. Z., Mullor, J. L., Casas, E., Allen, W. P., Gillessen-Kaesbach, G., Roeder, E. R., Ming, J. E., Altaba, A. R. and Muenke, M. 2003, *Proc. Natl. Acad. Sci. USA*, 100, 13424.
40. Bae, G. U., Domene, S., Roessler, E., Schachter, K., Kang, J. S., Muenke, M. and Krauss, R. S. 2011, *Am. J. Hum. Genet.*, 89, 231.
41. De Franco, E., Watson, R. A., Weninger, W. J., Wong, C. C., Flanagan, S. E., Caswell, R., Green, A., Tudor C., Lelliott, C. J., Geyer, S. H., Maurer-Gesek, B., Reissig, L. F., Allen, H. L., Caliebe, A., Siebert, R., Holterhus, P. M., Deeb, A., Prin, F., Hilbrands, R., Heimberg, H., Ellard, S., Hattersley, A. T. and Barroso, I. 2019, *Am. J. Hum. Genet.*, 104, 985.
42. Kruszka, P., Berger, S. I., Casa, V., Dekker, M. R., Gaesser, J., Weiss, K., Martinez, A. F., Murdock, D., Louie, R. J., Prijoles, E. J., Lichty, A. W., Brouwer, O. F., Zonneveld-Huijssoon, E., Stephan M. J., Hogue, J., Hu, P., Tanima-Nagai, M., Everson, J. L., Prasad, C., Cereda, A., Iascone, M., Schreiber, A., Zurcher, V., Corsten-Janssen, N., Escobar, L., Clegg, N. J., Delgado, M. R., Hajirnis, O., Balasubramanian, M., Kayserili, H., Deardorff, M., Poot, R. A., Wendt, K. S., Lipinski, R. J. and Muenke, M. 2019, *Brain*, 142, 2631.
43. Drissi, I., Fletcher, E., Shaheen, R., Nahorski, M., Alhashem, A. M., Lisgo, S., Fernandez-Jaen, A., Schon, K., Tlili-Graies, K., Smithson, S. F., Lindsay, S., Sharpe, H. J., Alkuraya, F. S. and Woods, G. 2022, *J. Med. Genet.*, 59, 358.
44. Sergi, C. and Kamnasaran, D. 2011, *Clin. Genet.*, 79, 293.
45. Erlich, M. S., Cunningham, M. L. and Hudgins, L. 2000, *Am. J. Med. Genet.*, 95, 269.
46. Tarantal, A. F. 2005, *The Laboratory Primate (Handbook of Experimental Animals)*. S. Wolfe-Coote (Ed.), Academic Press, Cambridge, 317.
47. Jeong, Y., El-Jaick, K., Roessler, E., Muenke, M. and Epstein, D. J. 2006, *Development*, 133, 76110.
48. Sagai, T., Amano, T., Maeno, A., Ajima, R., and Shiroishi, T. 2019, *Proc. Natl. Acad. Sci. USA*, 116, 23636.
49. Salama, G. S., Kaabneh, M. A., Al-Raqad, M. K., Al-Abdallah, I. M., Shakkoury, A. G. and Halaseh, R. A. 2015, *Clin. Med. Insights Pediatr.*, 9, 19.
50. Kruszka, P. and Muenke, M. 2018, *Am. J. Med. Genet. C. Semin. Med. Genet.*, 178, 229.
51. Roessler, E., Belloni, E., Gaudenz, K., Jay, P., Berta, P., Scherer, S. W., Tsui, L. C. and Muenke, M. 1996, *Nat. Genet.*, 14, 357.
52. Gill, S. K., Broussard, C., Devine, O., Green, R. F., Rasmussen, S. A., Reefhuis, J. and National Birth Defects Prevention Study. 2012, *Birth Defects Res. A. Clin. Mol. Teratol.*, 94, 1010.
53. Sikakulya, F. K., Kiyaka, S. M., Masereka, R. and Ssebuufu, R. 2021, *Case Rep. Otolaryngol.*, 2021, 7282283.
54. Cohen, M. M. Jr. and Shiota, K. 2002, *Am. J. Med. Genet.*, 109, 1.
55. Johnson, C. Y. and Rasmussen, S. A. 2010, *Am. J. Med. Genet. C. Semin. Med. Genet.*, 154C, 73.
56. Orioli, I. M. and Castilla, E. E. 2007, *Am. J. Med. Genet. A*, 143A, 3088.
57. Faye-Petersen, O., David, E., Rangwala, N., Seaman, J. P., Hua, Z. and Heller, D. S. 2006, *Fetal. Pediatr. Pathol.*, 25, 277.
58. Gekas, J., Li, B. and Kamnasaran, D. 2010, *Eur. J. Med. Genet.*, 53, 358.
59. Siebert, J. R., Astley, S. J. and Clarren, S. K. 1991, *Teratology*, 44, 29.
60. Tarantal, A. F. Otiang-a-Owiti, G. and Hendrickx, A. G. 1994, *J. Med. Primatol.*, 23, 319.
61. Byrne, P. J., Silver, M. M., Gilbert, J. M., Cadera, W., Tanswell, K., Reynolds, J. F.. 1987, *Am. J. Med. Genet.*, 28, 61.
62. Kilic, N. and Yazici, Z. 2005, *Int. J. Pediatr. Otorhinolaryngol.*, 69, 1275.
63. Yamasaki, M., Nomaka, M., Bamba, Y., Teromoto, C. M., Ban, C. and Pooh, R. K. 2012, *Semin. Fetal. Neonatal. Med.*, 17, 330.